Exact wave functions of electron in a quantum dot with account of the Rashba spin-orbit interaction

V. V. Kudryashov*
Institute of Physics, National Academy of Sciences of Belarus,
68 Nezavisimosti Ave., 220072, Minsk, Belarus

We present the exact wave functions and energy levels of electron in a two-dimensional circular quantum dot in the presence of the Rashba spin-orbit interaction. The confinement is described by the realistic potential well of finite depth.

PACS numbers: 03.65.Ge, 71.70.Ej, 73.21.La

The Rashba spin-orbit interaction in semiconductor quantum dots has been the object of many investigations in recent years (see [1, 2, 3, 4] and references therein). The Rashba interaction is of the form [5, 6]

$$V_R = \beta_R(\sigma_x p_y - \sigma_y p_x) \tag{1}$$

with standard Pauli spin-matrices

$$\sigma_x = \begin{pmatrix} 0 & 1 \\ 1 & 0 \end{pmatrix}, \quad \sigma_y = \begin{pmatrix} 0 & -i \\ i & 0 \end{pmatrix}. \tag{2}$$

The Rashba interaction can be strong in semiconductor heterostructures and its strength can be controlled by an external electric field.

The quantum dots in semiconductors can be described as effectively two-dimensional systems in confining potential $V_c(x,y)$. A confining potential is usually assumed to be symmetric, $V_c(x,y) = V_c(\rho), \rho = \sqrt{x^2+y^2}$. Then the single-electron wave functions satisfy the Schrödinger equation

$$\left(\frac{\mathbf{p}^2}{2\mu} + V_c(\rho) + V_R\right)\Psi = E\Psi, \tag{3}$$

where μ is the effective electron mass. There are two model potentials which are widely employed in this area. The first is a harmonic oscillator potential. Such a model [3, 4] admits the approximate (not exact) solutions of Eq. (3). The second model [1, 2] is a circular quantum dot with hard walls $V_c(\rho) = 0$ for $\rho < \rho_0$, $V_c(\rho) = \infty$ for $\rho > \rho_0$. This model is exactly solvable. In the framework of above models the number of allowed energy levels is infinite for the fixed total angular momentum.

In this paper, we examine a model which corresponds to a circular quantum dot with a rectangular potential well of finite depth: $V_c(\rho) = 0$ for $\rho < \rho_0$, $V_c(\rho) = V_0 > 0$ for $\rho > \rho_0$. We shall present the exact coordinate wave functions and energy levels for the wells of arbitrary depth.

The analogous model with replacement $V_c(\rho) \to V_c(\rho) - V_0$ was proposed in [7], where the approximate investigation was developed in the momentum representation for a shallow well. As to the coordinate representation, unfortunately the paper [7] does not contain the radial Schrödinger equations as well as the explicit and complete expressions for solutions of these equations. Emphasizing different aspects of the same problem the present paper and the paper [7] mutually complement each other.

The Schrödinger equation is considered in the cylindrical coordinates $x = \rho\cos\varphi, y = \rho\sin\varphi$. Further it is convenient to employ dimensionless quantities

$$e = \frac{2\mu}{\hbar^2}\rho_0^2 E, \quad v = \frac{2\mu}{\hbar^2}\rho_0^2 V_0, \quad \beta = \frac{2\mu}{\hbar}\rho_0\beta_R, \quad r = \frac{\rho}{\rho_0}. \tag{4}$$

As it was shown in [1], Eq. (3) permits the separation of variables:

$$\Psi_m(r,\varphi) = u(r)e^{im\varphi}\begin{pmatrix} 1 \\ 0 \end{pmatrix} + w(r)e^{i(m+1)\varphi}\begin{pmatrix} 0 \\ 1 \end{pmatrix}, \tag{5}$$

$$m = 0, \pm 1, \pm 2, \ldots$$

due to conservation of the total angular momentum $L_z + \frac{\hbar}{2}\sigma_z$.

In [1, 2], the requirements $u(1) = w(1) = 0$ were imposed. In the present model, we look for the radial wave functions $u(r)$ and $w(r)$ regular at the origin $r = 0$ and decreasing at infinity $r \to \infty$.

We consider two regions $r < 1$ (region 1) and $r > 1$ (region 2) separately.

In the region 1 ($v = 0$) the radial equations may be written in the suitable form

$$\begin{aligned} r^2\frac{d^2u_1}{dr^2} &+ r\frac{du_1}{dr} + (k_1^+k_1^-r^2 - m^2)u_1 \\ &= (k_1^+ - k_1^-)r^2\left(\frac{dw_1}{dr} + \frac{m+1}{r}w_1\right), \\ r^2\frac{d^2w_1}{dr^2} &+ r\frac{dw_1}{dr} + (k_1^+k_1^-r^2 - (m+1)^2)w_1 \\ &= -(k_1^+ - k_1^-)r^2\left(\frac{du_1}{dr} - \frac{m}{r}u_1\right), \end{aligned} \tag{6}$$

where

$$k_1^\pm(e,\beta) = \sqrt{e + \frac{\beta^2}{4}} \pm \frac{\beta}{2}. \tag{7}$$

*Electronic address: kudryash@dragon.bas-net.by

Note that in the case $\beta = 0$ ($k_1^+ = k_1^-$) Eqs. (6) are the Bessel equations. Therefore, following [1, 2] we use the known properties [8]

$$\begin{aligned}\left(\frac{d}{dr} - \frac{n}{r}\right) J_n(kr) &= -kJ_{n+1}(kr), \\ \left(\frac{d}{dr} + \frac{n}{r}\right) J_n(kr) &= kJ_{n-1}(kr) \end{aligned} \tag{8}$$

of the Bessel functions in order to obtain the exact solutions

$$\begin{aligned} u_1(m,e,\beta,r) &= c_1 f_1(m,e,\beta,r) \\ &+ d_1 g_1(m,e,\beta,r), \\ w_1(m,e,\beta,r) &= c_1 g_1(m+1,e,\beta,r) \\ &+ d_1 f_1(m+1,e,\beta,r) \end{aligned} \tag{9}$$

of system (6), where

$$\begin{aligned} f_1(m,e,\beta,r) &= \frac{1}{2}\left(J_m(k_1^- r) + J_m(k_1^+ r)\right), \\ g_1(m,e,\beta,r) &= \frac{1}{2}\left(J_m(k_1^- r) - J_m(k_1^+ r)\right) \end{aligned} \tag{10}$$

are the real linear combinations of the Bessel functions with real arguments. Here c_1 and d_1 are arbitrary coefficients. The radial wave functions $u_1(r)$ and $w_1(r)$ have the desirable behavior at the origin.

In the region 2 ($v > 0$) we have the radial equations

$$\begin{aligned} r^2\frac{d^2u_2}{dr^2} &+ r\frac{du_2}{dr} - (k_2^+ k_2^- r^2 + m^2)u_2 \\ &= -i(k_2^+ - k_2^-)r^2\left(\frac{dw_2}{dr} + \frac{m+1}{r}w_2\right), \\ r^2\frac{d^2w_2}{dr^2} &+ r\frac{dw_2}{dr} - (k_2^+ k_2^- r^2 + (m+1)^2)w_2 \\ &= i(k_2^+ - k_2^-)r^2\left(\frac{du_2}{dr} - \frac{m}{r}u_2\right), \end{aligned} \tag{11}$$

where

$$k_2^{\pm}(e,v,\beta) = \sqrt{v - e - \frac{\beta^2}{4}} \pm i\frac{\beta}{2}. \tag{12}$$

Now in the case $\beta = 0$ ($k_2^+ = k_2^-$) Eqs. (11) are the modified Bessel equations. Therefore, using the known properties [8]

$$\begin{aligned}\left(\frac{d}{dr} - \frac{n}{r}\right) K_n(kr) &= -kK_{n+1}(kr), \\ \left(\frac{d}{dr} + \frac{n}{r}\right) K_n(kr) &= -kK_{n-1}(kr) \end{aligned} \tag{13}$$

of the modified Bessel functions it is easily to get the exact solutions

$$\begin{aligned} u_2(m,e,v,\beta,r) &= c_2 f_2(m,e,v,\beta,r) \\ &+ d_2 g_2(m,e,v,\beta,r), \\ w_2(m,e,v,\beta,r) &= c_2 g_2(m+1,e,v,\beta,r) \\ &- d_2 f_2(m+1,e,v,\beta,r) \end{aligned} \tag{14}$$

of system (11), where

$$\begin{aligned} f_2(m,e,v,\beta,r) &= \frac{1}{2}\left(K_m(k_2^- r) + K_m(k_2^+ r)\right), \\ g_2(m,e,v,\beta,r) &= \frac{i}{2}\left(K_m(k_2^- r) - K_m(k_2^+ r)\right) \end{aligned} \tag{15}$$

are the real linear combinations of the modified Bessel functions with complex arguments. Here c_2 and d_2 are arbitrary coefficients. At large values of r the functions $f_2(m,e,v,\beta,r)$ and $g_2(m,e,v,\beta,r)$ behave as

$$\begin{aligned} f_2(m,e,v,\beta,r) &\sim \sqrt{\frac{\pi}{2}}\frac{1}{(v-e)^{1/4}} \\ &\times \frac{e^{-r\sqrt{v-e-\beta^2/4}}}{\sqrt{r}}\cos\left(\frac{\beta r + \gamma}{2}\right), \\ g_2(m,e,v,\beta,r) &\sim -\sqrt{\frac{\pi}{2}}\frac{1}{(v-e)^{1/4}} \\ &\times \frac{e^{-r\sqrt{v-e-\beta^2/4}}}{\sqrt{r}}\sin\left(\frac{\beta r + \gamma}{2}\right), \end{aligned} \tag{16}$$

where γ is defined as follows,

$$\cos(\gamma) = \frac{\sqrt{v - e - \beta^2/4}}{\sqrt{v-e}}, \quad \sin(\gamma) = \frac{\beta}{2\sqrt{v-e}}. \tag{17}$$

Thus, the radial wave functions $u_2(r)$ and $w_2(r)$ have the appropriate behavior at infinity. It should be noted that the radial wave functions have the infinite number of zeros for the finite value of energy.

Since the solutions (9) are valid for $e > -\beta^2/4$ and the solutions (14) are valid for $e < v - \beta^2/4$ then the complete energy range is $-\beta^2/4 < e < v - \beta^2/4$.

The continuity conditions

$$\begin{aligned} u_1(m,e,\beta,1) &= u_2(m,e,v,\beta,1), \\ u_1'(m,e,\beta,1) &= u_2'(m,e,v,\beta,1), \\ w_1(m,e,\beta,1) &= w_2(m,e,v,\beta,1), \\ w_1'(m,e,\beta,1) &= w_2'(m,e,v,\beta,1) \end{aligned} \tag{18}$$

for the radial wave functions and their derivatives at the boundary point $r = 1$ lead to the algebraic equations

$$M(m,e,v,\beta)\begin{pmatrix} c_1 \\ c_2 \\ d_1 \\ d_2 \end{pmatrix} = 0 \tag{19}$$

for coefficients c_1, c_2, d_1 and d_2, where

TABLE I: Energy levels.

v	β	e						
		$m=0$						
25	0	3.98	9.94	19.61				
25	1	3.49	9.81	19.15				
25	5	−4.40	2.83	13.40				
25	10	−23.25	−18.31	−9.67				
49	0	4.41	11.13	22.75	35.91			
49	1.4	3.49	11.03	21.87	35.79			
49	7	−10.40	−3.71	9.55	24.22			
49	14	−47.11	−41.45	−32.19	−19.60	−2.25		
100	0	4.77	12.09	24.97	40.08	60.28	81.84	
100	2	2.97	11.75	23.30	39.73	58.65	81.42	
100	10	−21.91	−16.95	−4.88	14.82	35.04	56.69	
100	20	−97.96	−91.83	−81.75	−67.58	−49.91	−28.53	−1.66
		$m=1$						
25	0	9.94	17.46					
25	1	9.02	17.85					
25	5	−2.52	9.26					
25	10	−23.22	−17.29	−4.85				
49	0	11.13	19.85	35.91				
49	1.4	9.41	20.50	34.28				
49	7	−9.62	1.84	20.95	36.73			
49	14	−47.04	−41.12	−31.51	−13.33			
100	0	12.09	21.66	40.08	57.25	81.84		
100	2	8.85	22.59	37.08	58.13	79.02		
100	10	−22.91	−14.79	4.24	31.61	55.83	74.93	
100	20	−97.91	−91.72	−81.26	−66.83	−48.24	−17.86	
		$m=2$						
25	0	17.46						
25	1	16.13						
25	5	1.30	16.08					
25	10	−22.86	−13.35	−0.20				
49	0	19.85	30.35					
49	1.4	17.37	31.72					
49	7	−6.88	10.11	32.20				
49	14	−44.83	−40.77	−26.05	−4.15			
100	0	21.66	33.34	57.25	76.20			
100	2	17.08	35.51	52.95	78.21			
100	10	−22.12	−8.70	16.99	49.86	74.91		
100	20	−97.84	−91.39	−80.29	−65.52	−37.69	−3.45	

$$M(m,e,v.\beta)=\begin{pmatrix} f_1(m,e,\beta,1) & -f_2(m,e,v,\beta,1) & g_1(m,e,\beta,1) & -g_2(m,e,v,\beta,1) \\ f_1'(m,e,\beta,1) & -f_2'(m,e,v,\beta,1) & g_1'(m,e,\beta,1) & -g_2'(m,e,v,\beta,1) \\ g_1(m+1,e,\beta,1) & -g_2(m+1,e,v,\beta,1) & f_1(m+1,e,\beta,1) & f_2(m+1,e,v,\beta,1) \\ g_1'(m+1,e,\beta,1) & -g_2'(m+1,e,v,\beta,1) & f_1'(m+1,e,\beta,1) & f_2'(m+1,e,v,\beta,1) \end{pmatrix}. \quad (20)$$

Hence, the exact equation for energy spectrum is

$$\det M(m,e,v,\beta)=0. \quad (21)$$

It should be stressed that in the explored model the num-

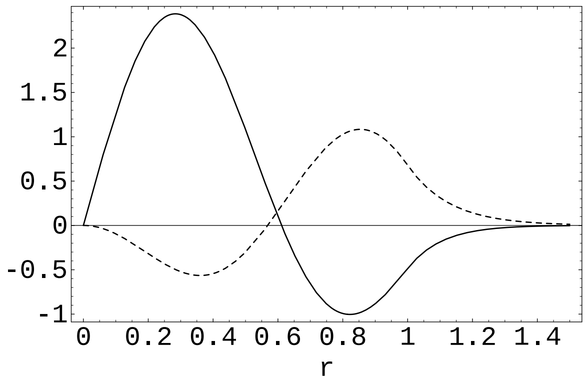

FIG. 1: Radial wave functions for $m = 1$. Solid line for $u(r)$, dashed line for $w(r)$.

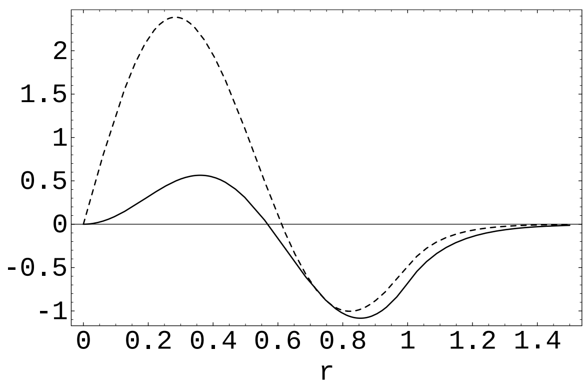

FIG. 2: Radial wave functions for $m = -2$. Solid line for $u(r)$, dashed line for $w(r)$.

ber of admissible energy levels is finite for the fixed total angular momentum. Note that Eq. (21) is invariant under two replacements $m \to -(m+1)$ and $\beta \to -\beta$.

If the energy values are found from Eq. (21) then it is simply to get the values of coefficients c_1, c_2, d_1 and d_2 from Eq. (19) and the following normalization condition $\int_0^\infty \left(u^2(r) + w^2(r)\right) rdr = 1$.

Now we present some numerical and graphic illustrations in addition to the analytic results.

Table I shows the dependence of energy e on the Rashba parameter β, the well depth v and angular momentum number m. The values of β are $0, 0.2\sqrt{v}, \sqrt{v}$ and $2\sqrt{v}$ for the given value of v. We see that the number of energy levels decreases if the well depth v decreases and if angular momentum number m increases. Besides we see that the negative energy values appear for the positive v when the values of β becomes sufficiently large in comparison with the value of $\sqrt{v}$. If $\beta^2/4 \geq v$ then the energy spectrum is completely shifted to negative region.

Figures 1 and 2 demonstrate the continuous radial wave functions for $m = 1$ and $m = -2$ respectively while $\beta = 2, v = 100$ and $e = 37.0825$ in both cases. The solid lines correspond to the functions $u(r)$ and the dashed lines correspond to the functions $w(r)$. The numerical values of coefficients are $c_1 = 4.22035, c_2 = -4067.87, d_1 = -0.7139284$ and $d_2 = 880.843$ in the case of Fig. 1 and $c_1 = 0.713928, c_2 = 880.843, d_1 = -4.22035$ and $d_2 = 4067.87$ in the case of Fig. 2. We see that the radial wave functions rapidly decrease outside the well. Figures indicate some symmetry properties of the radial wave functions under replacement $m \to -(m+1)$.

In our opinion the examined exactly solvable model with the realistic potential well of finite depth is physically adequate in order to describe the behavior of electron in a semiconductor quantum dot with account of the Rashba spin-orbit interaction. Further we intend to generalize our consideration by including the magnetic field effects on the orbital motion of electron in a quantum dot.

The author thanks K. Pankrashkin for pointing out the reference [7].

[1] E. N. Bulgakov and A. F. Sadreev, Pis'ma v ZhETF **73**, 577 (2001) [JETP Lett. **73**, 505 (2001)].
[2] E. Tsitsishvili, G. S. Lozano and A. O. Gogolin, Phys. Rev. **B70**, 115316 (2004).
[3] M. Valin-Rodriguez, Phys. Rev. **B70**, 033306 (2004).
[4] W. H. Kuan, C. S. Tang and W. Xu, J. Appl. Phys. **95**, 6368 (2004).
[5] E. I. Rashba, Fiz. Tverd. Tela (Leningrad) **2**, 1224 (1960) [Sov. Phys. Solid State **2**, 1109 (1960)].
[6] Yu. A. Bychkov and E. I. Rashba, J. Phys. **C17**, 6039 (1984).
[7] A. V. Chaplik and L. I. Magarill, Phys. Rev. Lett. **96**, 126402 (2006).
[8] M. Abramovitz and I. A. Stegun (eds.), *Handbook of Mathematical Functions* (Dover Publications, New York, 1970).